(28) Nystrom, B.; Bergman, R. *Eur. Polym. J.* **1978**, *14*, 431.
(29) Nystrom, B.; Roots, J.; Bergman, R. *Polymer* **1979**, *20*, 157.
(30) Nystrom, B.; Porsch, B.; Sundelof, L.-O. *Eur. Polym. J.* **1977**, *13*, 683.
(31) Nystrom, B.; Roots, J. *Eur. Polym. J.* **1978**, *14*, 551.
(32) Mijnlieff, P. F.; Jaspers, W. J. M. *Trans. Faraday Soc.* **1971**, *67*, 1837.
(33) Nystrom, B.; Sundelof, L.-O.; Bohdanecky, M.; Petrus, V. *J. Polym. Sci., Polym. Lett. Ed.* **1979**, *17*, 543.
(34) Nystrom, B.; Sundelof, L.-O. *Chem. Scr.* **1976**, *10*, 16.
(35) Nystrom, B.; Roots, J. *Makromol. Chem.* **1979**, *180*, 2419.
(36) Tirrell, M. *Rubber Chem. Technol.* **1984**, *57*, 523.
(37) Lin, T.-H.; Phillies, G. D. J. *J. Colloid Interface Sci.* **1984**, *100*, 82.

Thermodynamic Studies on Poly[*N*-(*n*-octadecyl)maleimide] (PMI-18)/Solvent Systems by Inverse Gas Chromatography with Capillary Columns†

J. M. Barrales-Rienda* and J. Vidal Gancedo

Instituto de Plásticos y Caucho, C.S.I.C. Juan de la Cierva, 3, 28006 Madrid, Spain.
Received January 5, 1987

ABSTRACT: An open tubular column (capillary) coated with poly[*N*-(*n*-octadecyl)maleimide] (PMI-18) has been used above its glass transition temperature for estimating polymer–solvent interaction parameters by means of inverse gas chromatography (IGC). Experimental retention volumes corrected to zero flow rate V_g^0 are reported for nonpolar (C_n *n*-alkanes, n = 9–13) and polar (C_n *n*-alkyl alcohols, n = 6–8 and 10) solute probes. Activity coefficients $(a_1/\omega_1)^\infty$, the Flory–Huggins parameter χ, and mixing functions were derived and discussed with respect to the chain length and polarity in the solute molecules. The heat of mixing at infinite dilution $\Delta\bar{H}_1^\infty$ taken at the midpoint, 143 °C, is in the range of 60 to 160 J/g. These values are interpreted as indicative of some fitting of a cooperative orientational order between neighboring *n*-alkyl side chains of a comb structure and the *n*-alkyl side of the probe molecules. The heats of vaporization of solute molecules, ΔH_v, are in quantitative agreement with those calculated from vapor pressures by means of the Clausius–Clapeyron equation. The apparent glass transition temperature, T_g, estimated by IGC was found to be dependent on the chemical nature of the probe and the number of methylene groups in the *n*-alkyl chain. This dependence is explained within the framework of the theory of free volume and the difussion coefficient of the probe molecules into the polymer by an equation of the Fujita type. An expression has been derived from the free volume theory which relates the self-diffusion coefficient of the probes in the gaseous state to the apparent glass transition temperature of the PMI-18 estimated by IGC.

Introduction

A few years ago, Lichtenthaler and Prausnitz[1,2] reported the use of open tubular capillary columns to measure polymer–solute interaction parameters by inverse gas–liquid chromatography (IGC). The only reason given by these authors[1,2] for the employment of open tubular (capillary) over packed columns was to provide an increase in film thickness, thus simulating the conditions prevailing in the bulk material. Since then very little attention has been paid to the study of IGC by means of open tubular columns. Latter, Braun and Guillet[3] concluded that the film thickness in packed columns may be only an order of magnitude less than for capillary columns. They also claimed that due to high linear velocities of carrier gas and thick polymer films, the retention data in the case of capillary columns must be obtained from lengthy and necessarily less precise extrapolation procedures.[3] However, they did not present any experimental fact in favor of their arguments.

Interlaboratory comparison of retention data obtained on packed columns has indicated that column packing procedures may be of fundamental importance.[4] However, very recently, Card, Al-Saigh, and Munk[5] carried out a detailed study on the role played by the very often termed "*innert support*" by studying retention volumes of nonpolar as well as moderately and strongly polar probes. They concluded that to obtain meaningful data for the retention of the probes and the thermodynamic parameters derived from the retention volumes, the data measured on the uncoated column support had to be subtracted from the corresponding data of the coated column support.

In addition, open tubular columns have rarely been used for thermodynamic measurements. The data on the Flory–Huggins parameter χ obtained from a packed column according to Lichtenthaler et al.[1] are lower than static data. However, the differences are less if the comparison is made between data from static experiments and those from capillary columns.

In the present paper we have focused our main interest on the three following points: (i) We explored the validity of the data obtained by using open tubular columns coated on the inner wall with a polymer above its glass transition temperature and extrapolated the retention volume to zero flow rate. (ii) The study of the influence of a comb structure such as the poly[*N*-(*n*-octadecyl)maleimide] by using both nonpolar (*n*-alkanes) and polar (*n*-alkyl alcohols) substances as probes on the thermodynamic properties of mixing was conducted. In linear polymers these thermodynamic functions are determined by interactions between the solvent molecule and short sequences within the polymer chain. A thermodynamic study of polymer–probe interactions can lead to an understanding of the specific interaction between the probe molecules and the polymer structure. (iii) We examined the dependence of the glass transition temperature determined by IGC on the structural properties and dimensions of *n*-alkyl derivatives used as probes.

Experimental Section

The experimental framework of IGC is mainly in the literature, so that only the significant details will be covered here. Experimental procedures on IGC in general[5-9] and open tubular columns in particular[1,2,10] will be used.

Materials. A fractionated sample of PMI-18 of $\bar{M}_n = 1.90 \times 10^5$ and $\bar{M}_w/\bar{M}_n = 1.74$, as estimated from measurements by

† Dedicated to Professor Dr. A. P. Masiá on the occasion of his 63rd birthday.

0024-9297/88/2221-0220$01.50/0

membrane osmometry and gel permeation chromatography using a self-calibration method[11] and T_g = 386.5 K estimated by DSC at the null rate of heating,[12] was used.

PMI-18 is a typical comblike polymer with structural unit I.

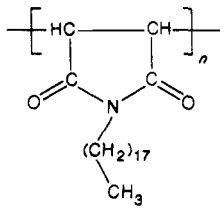

I

Reagent grade solutes, C_n *n*-alkanes (n = 9–13) and C_n *n*-alkyl alcohols (n = 6–8 and 10), were used without further purification (Merck, A. G., Fluka, A. G., and Carlo Erba, S.p.A.).

Preparation of Column. Different methods have already been described in detail for preparing capillary columns. Preparation of open tubular columns by the solvent plug technique and their utilization has been discussed and described in detail by Ettre,[13] Lichtenthaler and Prausnitz,[1,2,4] and Gray and Guillet.[10]

A stainless steel column, i.d. 0.050 cm, 25 m long, with a wall thickness of 0.0125 cm (S.G.E. 25 SSB/BM) was used. The column was cleaned up following instructions given by Mon.[14]

A reservoir containing measured amounts of a PMI-18 fraction dissolved in THF (1.28×10^{-2} g/mL) was attached to the column and kept in a vacuum oven. The solvent was evaporated slowly at moderately reduced pressure, 20 mmHg below atmospheric pressure, with moderate heating (40 °C) and frequent and intermittent changes of position to prevent inhomogeneous deposition of the polymer film. It was heated for 48 h at 150 °C under high-vacuum conditions (0.01 mmHg) to remove any trace of THF.

The amount of polymer in the column was determined by careful weighing to constant weight after complete drying under constant flow of helium at 150 °C. The resulting film thickness for our column assuming homogenous distribution was 1.67×10^4 Å. The column was conditioned overnight with helium in the GC instrument at 170 °C and then cooled at about 0.5 °C/min to room temperature before each use in order to allow the polymer the same thermal history. Solvent sample size was kept as small as possible ($\ll$0.05 μL).

Instrumentation. A Perkin-Elmer Model 3920 B gas chromatograph equipped with a Perkin-Elmer Model 3920 thermal conductivity detector was modified to include a very precise flow control and pressure manometer on the carrier gas inlet. Oven temperature was measured to the nearest 0.1 °C by using a precision quartz thermometer (Hewlett-Packard Model HP 2804 A) with a sound probe (Hewlett-Packard quartz probe Model 18111 A) which was inserted into the oven chamber through a 10-mm-diameter hole drilled through the oven cover. It was sealed with two pieces of Teflon ferrule of 5-mm inner diameter and 5.5-cm length.

The positions of peak maxima in some cases were obtained from the recorded graphs of the elution peak by a method[9] similar to that employed by Pella and Nebuloni[15] to locate melting point maxima in DSC traces.

Primary Data Reduction. Equations 1, 2, and 3 were used to obtain V_g^0, the specific retention volume (corrected to 0 °C and zero flow rate),[16] $(a_1/\omega_1)^\infty$, the weight fraction activity coefficient at infinite dilution,[17] and χ, the residual free energy of interaction between solute and polymer for high molecular weight polymer, respectively. V_g is obtained by

$$V_g = \Delta t_r(F/w_2)(3/2)[(p_i/p_o)^2 - 1][(p_i/p_o)^3 - 1]^{-1} \times (1 - (p_{H_2O}/p_a)) \quad (1)$$

where $\Delta t_r = t_p - t_m$ is the difference between retention time of the probe t_p and of the marker t_m. F is the flow rate of carrier gas measured at room temperature with a soap bubble flow meter at ambient temperature p_a, w_2 is the mass of the polymer in the column, p_i and p_o are the inlet and outlet pressures, respectively, and p_{H_2O} is the water vapor pressure at room temperature. Retention volumes were corrected to zero flow rate V_g^0. The flow dependence of the specific retention volume for the PMI-18/*n*-decane system at several temperatures is shown in Figure 1. The activity coefficient is obtained from

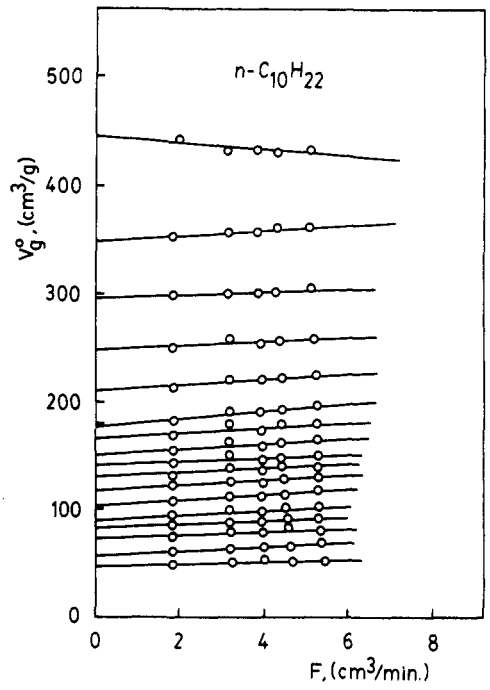

Figure 1. Effect of the flow rate on the specific retention volume V_g^0 for the poly[*N*-(*n*-octadecyl)maleimide] (PMI-18)/*n*-decane system at different temperatures. Some experimental data have been omitted for simplicity.

$$\ln \Omega_1^\infty = \ln (a_1/\omega_1)^\infty = \ln (273.2R/p_1^0V_g^0M_1) - (p_1^0/RT)(B_{11} - V_1) \quad (2)$$

where V_1, M_1, and p_1^0 refer to the solute molar volume, molecular weight, and saturated vapor pressure, R is the gas constant, T is the column temperature (K), and B_{11} the second virial coefficient to correct for vapor-phase nonideality of the probe.

At infinite dilution of the probe and for high molecular weight of the polymer, the Flory–Huggins residual free energy of interaction between solute and polymer χ is determined from

$$\chi = \ln (273.2R\nu_2/V_g^0p_1^0V_1) - 1 - p_1^0(B_{11} - V_1)/RT \quad (3)$$

where ν_2 is the specific volume of the polymer. Solute vapor pressures were computed from the Antoine equation,

$$\log p_1^0 = A - B/(C + t) \quad (4)$$

where t is the temperature (°C) and A, B, and C are constants which have been taken from the literature.[18]

Solute densities were obtained from Orwoll and Flory[19] and Timmermans[20] for *n*-alkanes and from Costello and Bowden[21] for *n*-hexyl alcohol, *n*-octyl alcohol, and *n*-decyl alcohol and from ref 22 for *n*-heptyl alcohol.

Second virial coefficients for *n*-alkanes (B_{11}) were computed from the following expression:[23]

$$B_{11}/\bar{V}_c = 0.430 - 0.886(T_c/T) - 0.694(T_c/T)^2 - 0.0375(n - 1)(T_c/T)^{4.5} \quad (5)$$

where V_c and T_c are critical volumes and temperatures, T is the temperature (K), and n is the number of carbon atoms of the *n*-alkane. Critical constants were taken from tables given by Dreisbach.[24]

The second virial coefficient for *n*-alkyl alcohols has been calculated from the expression given by Pitzer and Curl,[25]

$$B_{11}P_c/RT_c = (0.1445 + 0.073\omega) - (0.330 - 0.46\omega)T_r^{-1} - (0.1385 + 0.50\omega)T_r^{-2} - (0.0121 + 0.097\omega)T_r^{-3} - 0.0073\omega T_r^{-8} \quad (6)$$

in which ω is known as an acentric factor defined by

$$\omega = -\log (P_s/P_c) - 1.000 \quad (7)$$

and P_s is defined as the vapor pressure at $T_r = T_s/T_c = 0.700$.

Table I
Thermodynamic Interaction Parameters for PMI-18 and *n*-Alkanes and *n*-Alkyl Alcohols at Infinite Dilution

	130 °C		140 °C		150 °C		160 °C		170 °C	
solute	$(a_1/\omega_1)^\infty$	χ	$(a_1/\omega_1)^\infty$	χ	$(a_1/\omega_1)^\infty$	χ	$(a_1/\omega_1)^\infty$	χ	$(a_1/\omega_1)^\infty$	χ
					n-Alkanes					
n-nonane	5.21	0.269	4.84	0.191	4.58	0.128	4.25	0.068	4.45	0.084
n-decane	4.90	0.235	4.54	0.154	4.29	0.089	4.02	0.019	4.51	−0.042
n-undecane	4.36	0.133	4.01	0.042	3.77	−0.024	3.40	−0.134	3.75	−0.206
n-dodecane	4.23	0.123	3.94	0.048	3.68	−0.025	3.37	−0.116	3.26	−0.157
n-tridecane	4.18	0.122	3.86	0.039	3.61	−0.030	3.33	−0.114	3.26	−0.185
					n-Alkyl Alcohols					
n-hexyl alcohol	4.45	0.270	4.01	0.161	3.60	0.049	3.27	−0.054	3.03	−0.137
n-heptyl alcohol	4.33	0.246	3.91	0.136	3.52	0.028	3.25	−0.057	3.03	−0.132
n-octyl alcohol	4.13	0.202	3.79	0.114	3.46	0.018	3.12	−0.089	2.92	−0.160
n-decyl alcohol	3.74	0.114	3.47	0.035	3.19	−0.050	2.99	−0.119	2.88	−0.161

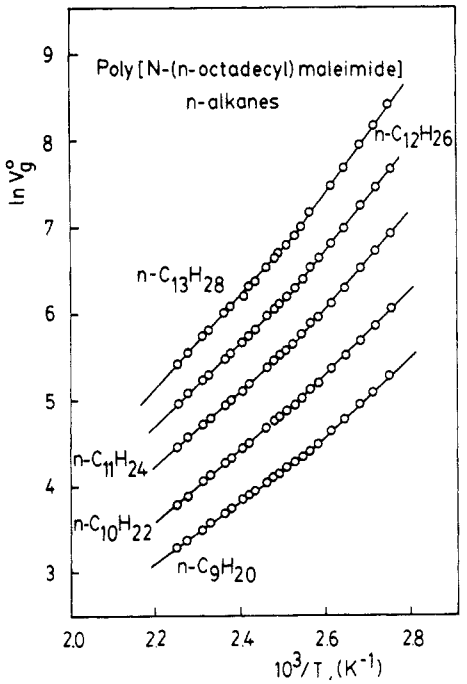

Figure 2. Specific retention diagrams for *n*-alkanes on PMI-18 as a function of reciprocal temperature. V_g^0 represents specific retention volumes corrected at zero flow rate.

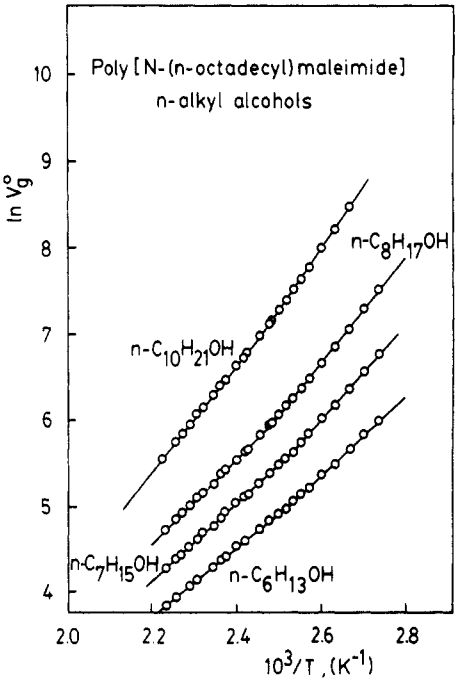

Figure 3. Specific retention diagrams for *n*-alkyl alcohols on PMI-18 as a function of reciprocal temperature. V_g^0 represents specific retention volumes corrected at zero flow rate.

Equation 7 only needs critical magnitudes for its application. However, it gives a higher accuracy on the values estimated for B_{11} than those from the Berthelot equation.

Specific volume of the polymer was calculated from volumetric data[26] for unfractionated PMI-18,

$$\nu_2\ (\mathrm{cm^3/g}) = 1.042 + [T(\mathrm{K}) - 348]\ 8.75 \times 10^{-4} \qquad (8)$$

where 8.75×10^{-4} represents $\Delta\alpha = \alpha_l - \alpha_g$ for PMI-18.

Results and Discussion

The flow rate dependence of the specific retention volume V_g is shown in Figure 1 for the PMI-18/*n*-decane system at several temperatures. Equation 1 was used to calculate the peak maximum retention volumes. Straight lines were obtained for all the systems studied in this work. In every case a linear extrapolation to zero flow rate gave a good representation of the experimental data. V_g^0's are actually extrapolated values by linear extrapolation to zero flow rate. Values of $(a_1/\omega_1)^\infty$, calculated by means of eq 2 and given at some temperatures in Table I, are in the range 2–5. Low values are indicative of polymer–solute miscibility, whereas values greater than 5 are characteristic of poor polymer/solvent systems.

Values of the residual free energy of interaction of Flory–Huggins[27,28] χ range from 0.3 to −0.2. In order to attain good polymer–solute miscibility, χ must be less than the critical value of 0.5.[27,28]

It is apparent from comparison of the χ values that the *n*-alkanes, in general, are slightly less soluble in PMI-18 than *n*-alkyl alcohols. In fact *n*-alkyl alcohols tend to dissolve PMI-18; they are Θ-solvents above room temperature[29] (see sixth column of Table III).

However, these results indicate that the presence of a hydroxyl group in the probe is not so important as expected in determining miscibility with PMI-18.

This may be due to some kind of association between the *n*-alkyl side chains and probe molecules, i.e., orientation correlations between *n*-alkyl side chains and their interaction with solvent molecules.[29] The *n*-alkyl part of *n*-alkanes and *n*-alkyl alcohols is probably responsible for such a specific interaction. These results are in excellent agreement with the values obtained for the partial molar heats of mixing $\Delta\bar{H}_1^\infty$ as will be shown below.

The same trend in the ln V_g^0 versus $1/T$ plots shown in Figures 2 and 3 has been found for some other systems. Thus, Braun and Guillet[30,31] studied the effect of coating thickness in packed columns on the polystyrene/*n*-hexadecane system. They found considerable changes in the shape of the retention diagrams by changing the loading from the sigmoidal-type curves to a diagram where the ln V_g^0 versus $1/T$ over the entire range can be conveniently represented by two intersecting straight lines corresponding to two very well differentiated regimes. At low

Table II
Partial Molar Heat of Mixing, Heat of Solution, and Heat of Vaporization of Several *n*-Alkanes and *n*-Alkyl Alcohols in Poly[*N*-(*n*-octadecyl)maleimide] (PMI-18)

solute	temp range, °C	$\Delta\bar{H}_1^\infty$, cal/mol (eq 10)	$-\Delta H_s$, cal/mol (eq 11)	ΔH_v, cal/mol (eq 12)
		n-Alkanes		
n-nonane	120–170	1927	7379	9306
n-decane	122–170	1577	8664	10242
n-undecane	122–170	2147	9058	11206
n-dodecane	116–170	2508	9642	12150
n-tridecane	116–170	2409	10728	13136
		n-Alkyl Alcohols		
n-hexyl alcohol	118–170	4066	7510	11578
n-heptyl alcohol	118–170	3045	9339	12384
n-octyl alcohol	124–170	2805	10354	13159
n-decyl alcohol	127–170	2248	12578	14827

enough loading the crossing point was no longer detectable. This happens for a loading of 0.36% and an average thickness of 60 Å. It also happens with systems such as polystyrene/perfluoro-*n*-eicosane,[32] polystyrene/nitromethane,[33] poly(*N*-isopropylacrylamide)/*n*-butyl alcohol,[32] polyethylene/cyclopentane,[7] and poly(stearyl methacrylate)-*graft*-poly(methyl methacrylate) copolymer/*n*-dodecane.[34] Some possible explanations have been given in terms of Martin's equation.[35]

It is clear that changes in retention behavior can be due to a change in surface to volume (mass) of the polymer and its influence on the combined surface and bulk retention mechanism apart from the method used to prepare the column and thermal history. For this reason, the total retention volume can be expressed as a function of four main factors, the partition coefficient due to surface adsorption K_{AD}, the partition coefficient due to bulk absorption K_{AB}, the available surface area of the polymeric coating S, and its mass m. They are related by means of Martin's equation,[30,35]

$$V_g^0 = K_{AD}(S/m) + K_{AB} \tag{9}$$

Under the experimental condition of our open tubular column the high load and low surface area make the ratio S/m almost negligible and therefore $K_{AB} \gg K_{AD}(S/m)$. In other words V_g^0 is controlled by K_{AB}. This means that our system follows an equilibrium bulk absorption mechanism not only above but also below T_g. So in this case the polymer morphology may play an important role. Therefore a change in the ln V_g^0 versus $1/T$ slope is indicative of different heats of solution for a given solute in the same polymer depending on the structure of the polymeric matrix. This condition is fulfilled by our comb structure.

The partial molar heat of mixing, $\Delta\bar{H}_1^\infty$, of the solute at infinite dilution in the polymer is given by

$$\Delta\bar{H}_1^\infty = R\delta(\ln (a_1/\omega_1)^\infty)/\delta(1/T) \tag{10}$$

therefore $\Delta\bar{H}_1^\infty$ may be obtained from the slope of the best straight line through a plot of the logarithm of the activity coefficient versus the reciprocal of the absolute temperature, as determined by a linear least-squares analysis. A linear temperature dependence was obtained for all systems studied.

Heats of solution, ΔH_s, were determined in a similar manner from the temperature dependence of the specific retention volumes,

$$\Delta H_s = -R\delta(\ln V_g^0)/\delta(1/T) \tag{11}$$

Values for $\Delta\bar{H}_1^\infty$ and ΔH_s are gathered in Table II. Heats of vaporization for the solutes (at 143 °C) were obtained from the heats of solution and heats of mixing in Table II as follows:[36]

$$\Delta H_v = \Delta\bar{H}_1^\infty - \Delta H_s \tag{12}$$

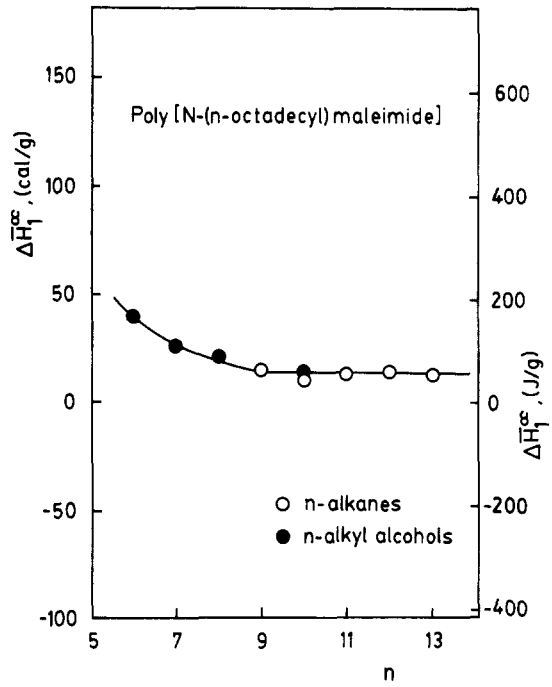

Figure 4. Comparison of $\Delta\bar{H}_1^\infty$ (cal/g or J/g) for two homologous series of probes on PMI-18 versus the number of carbon atoms of the *n*-alkyl chain of the probe.

Table II gives the values of $\Delta\bar{H}_1^\infty$, ΔH_s, and ΔH_v for all the systems studied. In figure 4, $\Delta\bar{H}_1^\infty$ has been plotted against the carbon atom number of the n-alkyl chain. Data for *n*-alkanes and *n*-alkyl alcohols have been plotted side by side to show clearly the analogies between probes of different chemical functionality and *n*-alkyl length. Both series of compounds are clearly situated along the same line. It is believed that heats of mixing in *n*-alkane systems may reflect correlations of molecular orientations.[37] Since interactions between aligned chains are energetically more favorable than between randomly oriented chains, an ordered phase becomes thermodynamically more stable than a nonordered one.[38] As can be seen on Figure 4 there is no significant increase of $\Delta\bar{H}_1^\infty$ for longer *n*-alkanes. They are in the range 60–160 J/g. Two superimposed trends are observed: one for *n*-alkyl alcohols where there is a smooth dependence between $\Delta\bar{H}_1^\infty$ and the number of carbon atoms in the *n*-alkyl chain; the other for *n*-alkanes where $\Delta\bar{H}_1^\infty$ remains constant all over the range. At least in the range of C_n studied in these two homologous series, we may conclude that from $n = 9$, $\Delta\bar{H}_1^\infty$ does not depend on probe molecule length. However, any reduction of the *n*-alkyl alcohol length would lead to an increase of $\Delta\bar{H}_1^\infty$. These findings, we believe, are due to a chain length effect more than to the different character of the polymer–solvent interaction.

Comparison of $(a_1/\omega_1)^\infty$ and χ values (Table I) for the *n*-alkanes with those for *n*-alkyl alcohols at equal chain length demonstrates that the presence of a hydroxyl group in the *n*-alkyl alcohol molecules does not promote any change in the intermolecular interactions. This suggests that the interaction with *n*-alcohols should be caused by the *n*-alkyl chain side.

It should be mentioned that the order of comblike polymer in bulk, concentrate, and dilute solution are identical. Thus, crystallization and layer ordering in the melt, layer ordering in gel solutions, and order tendency

Table III
Molar Volumes V_1, Flory–Huggins Residual Free Energy Parameter χ, and Solubility Parameter for the Probes at 143 °C and Apparent Glass Transition Temperature T_g, Θ Temperature, Collision Diameters σ, and Diffusion Coefficient $D(T)$ for the Systems PMI-18/*n*-Alkanes and PMI-18/*n*-Alkyl Alcohols

solute	V_1, cm³/mol	χ	δ_1, cal$^{1/2}$/cm$^{3/2}$	T_g, °C	Θ, °C	σ, Å	$D(T) \times 10^6$, cm²/s
			n-Alkanes				
n-nonane	208.4	0.177	6.35	117.5		6.06[b]	1.67
n-decane	225.0	0.139	6.47	119.5		6.19[b]	1.53
n-undecane	243.6	0.018	6.53	122.5		6.24[b]	1.44
n-dodecane	259.4	0.025	6.62	123.5		6.31[b]	1.35
n-tridecane	277.4	0.020	6.66	125.0		6.32[b]	1.30
			n-Alkyl Alchols				
n-hexyl alcohol	141.5	0.133	8.71	118.5	78.0	6.10[c]	1.86
n-heptyl alcohol	165.9	0.113	8.48	119.5	65.1[a]	6.43[c]	1.57
n-octyl alcohol	178.8	0.076	8.30	122.0	53.7	6.65[c]	1.38
n-decyl alcohol	214.9	0.014	8.07	126.0	39.3	7.24[c]	1.07

[a] Calculated by means of Θ (K) = $5.61 \times 10^2\, n^{-0.26}$ from ref 29. [b] Calculated by means of eq 25 and 26. [c] Calculated by means of eq 27 and 28. A mean value of 1.60 D for the dipole moment of every *n*-alkyl alcohol has been taken due to the scattering given in the literature[54] for this magnitude. The precise value of μ (1.0–2.0 D) does not affect too much the final result for δ and therefore σ.

in dilute solution of comblike polymers are due to strong intra- and intermolecular interactions by means of an orientational ordering in the side chains.[39] From this point of view the above behavior (Figure 4) of our comb structure in solvents of similar structure to the side chain may be easily explained assuming a highly ordered system from the point of view of molecular organization between the *n*-alkyl side chain of our PMI-18 and *n*-alkanes and *n*-alkyl alcohols.

Most of characteristic properties for comblike polymers with sufficiently long (C_n, $n = 6$) *n*-alkyl side chain are determined in many respects by interaction of side chains. The parallel type of packing of the side chains may create favorable conditions for the contact of the probe molecules. One of the ends of the *n*-alkyl chain is fixed to the main chain. Thus there is a restriction when an *n*-alkyl side chain is compared to a normal n-alkane. These orientational contacts are so important that the gels from comblike polymers and *n*-alkanes or *n*-alkyl alcohols exhibit remarkable stability; no phase separations take place even for some years. Finally, the cooperative orientational order between neighboring *n*-alkyl side chains of the polymer and the *n*-alkyl side of our probe molecules may explain the order of magnitude observed for $\Delta\bar{H}_1^\infty$ as well as the trend shown in the range of *n* from 6 to 13 depicted in Figure 4. In addition, the cooperative orientational order or alignment of *n*-alkyl side chains of PMI-18 seems to be easier with short-chain *n*-alkyl alcohol molecules. Our results agree with those found by Phuong-Nguyen and Delmas[40] for linear atactic polymers such as polybutadiene and polypentenamer and *n*-alkanes. They found values for $\Delta\bar{H}_1^\infty$ of 4–5 and 2–3 J/g, respectively. These values are interpreted as indicative of some fitting of the orientational order between segments of the polybutadiene and polypentenamer and *n*-alkanes.

Whether the ΔH_v is calculated from IGC data via eq 12 or estimated by means of the Clausius–Clapeyron equation from vapor pressure versus temperature data, equivalent results are obtained. To check this agreement we show in Figure 5 calculated values according to eq 12 (ordinate) plotted versus ΔH_v from the Clausius–Clapeyron equation (abscissa). The points are distributed more or less along the line of the ΔH_v(ordinate) = ΔH_v(abscissa) diagonal. The agreement is quite good in spite of the calculation done to estimate ΔH_v by means of eq 10–12.

Solubility parameters, δ_1, were calculated for the various *n*-alkanes and *n*-alkyl alcohols from the relation

$$\delta_1 = [(\Delta H_v - RT)/V_1]^{1/2} \tag{13}$$

where R is the universal gas constant and V_1 is the solute molar volume corresponding to temperature T (K), which was chosen as the midpoint of the temperature range investigated for our poly[*N*-(*n*-octadecyl)maleimide] (416.2 K); ΔH_v is the molar enthalpy of vaporization for the solute at temperature T. The use of ΔH_v calculated through the eq 12 from IGC data or by means of ΔH_v estimated from the Clausius–Clapeyron equation does not affect the final results on δ_1 for the probes. Calculated values of δ_1 at 416.16 K are summarized in Table III.

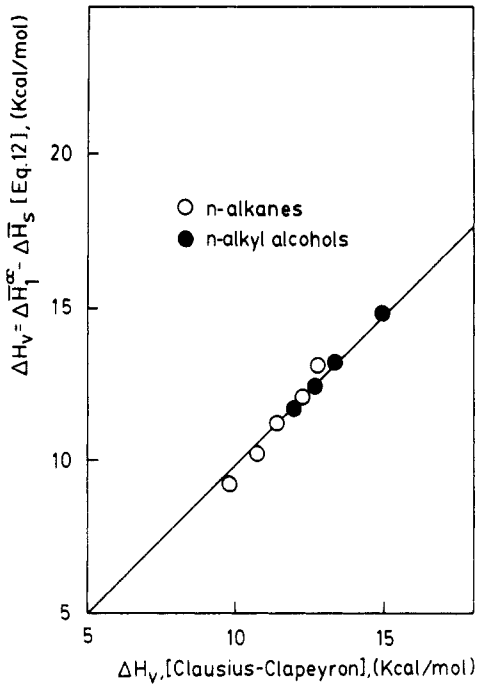

Figure 5. Comparison of experimental data for ΔH_v versus ΔH_v calculated according to the Clausius–Clapeyron equation. The full line represents the bisecting line for ΔH_v(eq 12) = ΔH_v-(Clausius–Clapeyron) for two homologous series of *n*-alkanes and *n*-alkyl alcohols.

A procedure for estimating the solubility parameter of a polymer is to combine the Flory treatment[41] with Hildebrand-Scatchard[42] theory to give the following relationship for the interaction parameter,[42] χ:

$$\chi = (V_1/RT)(\delta_1 - \delta_2)^2 \tag{14}$$

This equation can be rewritten as

$$\left[\frac{\delta_1^2}{RT} - \frac{\chi}{V_1}\right] = \frac{2\delta_2}{RT}\delta_1 - \frac{\delta_2^2}{Rt} \tag{15}$$

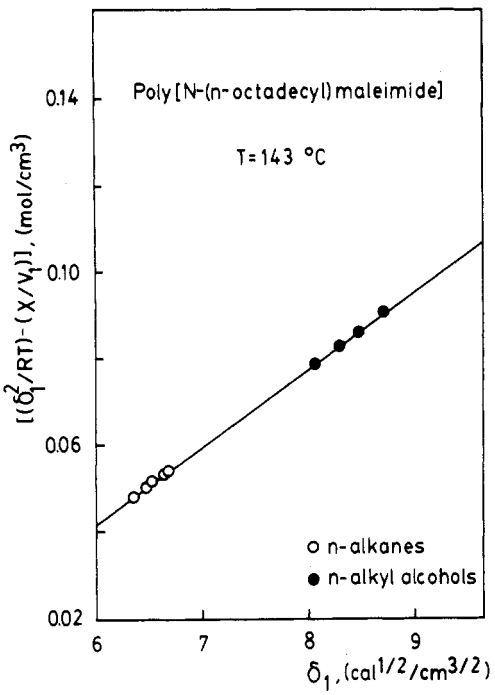

Figure 6. Estimation of solubility parameter (δ_2) of PMI-18 from δ_1 (solubility parameter of the probes) and χ (residual free energy of interaction) parameters at 143 °C.

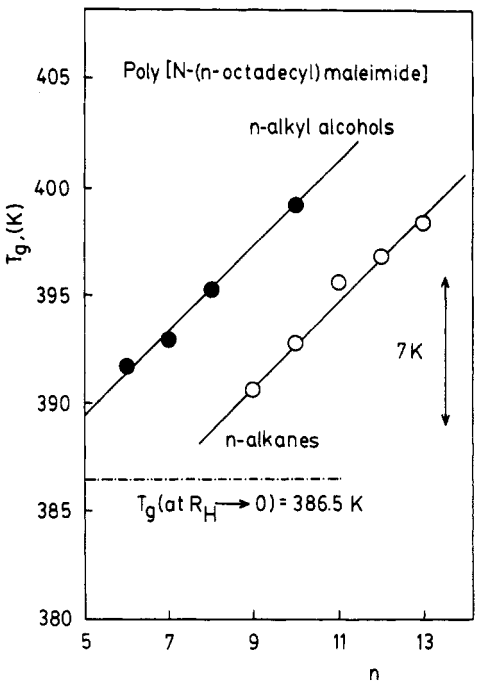

Figure 7. Dependence of apparent glass transition temperature of PMI-18 on the number of carbon atoms in *n*-alkanes and *n*-alkyl alcohols used as molecular probes.

Therefore a plot of $[(\delta_1^2/RT) - (\chi/V_1)]$ versus δ_1 of probes should yield a straight line with a slope of $2\delta_2/RT$ and an intercept of $-\delta_2^2/RT$. The polymer solubility parameter δ_2 thus obtained for PMI-18 at 143 °C corresponds to the midpoint of temperature range investigated. The results are illustrated in Figure 6. An excellent linear correlation is found. The slope and intercept were obtained from a linear least-squares analysis. Both the *n*-alkanes and *n*-alkyl alcohols lie on the same line and therefore yield the same values for the solubility parameter. For this reason we may conclude that the polymer solubility parameter δ_2 is independent of the chemical structure of the probe and its solubility parameter. Derived values of δ_2 at 143 °C for the PMI-18 are 7.41 and 7.44 cal$^{1/2}$/cm$^{3/2}$ from the intercept and the slope, respectively. This means that in applying eq 15 the δ_2 values derived from the slope and intercept are consistent. So it is easily concluded that eq 15 provides a useful method for estimating the solubility parameter of a polymer δ_2 at infinite dilution in the probe solvent by using IGC data.

Figures 2 and 3 also illustrate the retention diagrams that have been used to derive apparent glass transition temperatures values for PMI-18/*n*-alkanes and *n*-alkyl alcohols. The value of T_g is located at the point where the plot of ln V_g^0 versus $1/T$ departs from linearity. Very often this departure is followed by an inflection with sigmoidal shape. However, in some cases only a change in shape has been observed as has been mentioned above. Now it is well established that sigmoidal-type retention diagrams are related to a transition of surface to bulk retention mechanism in the vicinity of T_g in the polymeric stationary phase.[33] In a few other cases total linear retention diagrams, corresponding to surface adsorption, were recorded through T_g. This was attributed to the impossibility for a nonsolvent to penetrate to bulk polymer, even at temperature above T_g.[43]

In our case each one of the lines of Figures 2 and 3 is characterized by a single and well-defined value for T_g, given in Table III and shown in Figure 7. It can be seen that the addition of each methylene group increases T_g in a linear manner for each one of the two homologous series of *n*-alkanes and *n*-alkyl alcohols employed as probes. The value ΔT_g per methylene group CH_2 is equal to 2 K for *n*-alkanes and *n*-alkyl alcohols.

The same behavior has also been found by Belousov et al.[44] for poly(carbonate), a poly(sulfone), and poly(methyl methacrylate) as polymers and *n*-alkanes as probes. They explain this behavior assuming that the diffusion of sample and solute molecules into the polymer matrix starts when the average size of the holes, as a result of which overall free volume is implanted, agrees with the size of sample molecules. According to Braun and Guillet,[31] at temperatures above T_g, where equilibrium conditions can no longer be sustained, the penetration of the solute molecules in the bulk of the polymer is incomplete and the fractional value of the matrix accesible to the probe increases with temperature at a rate proportinal to the square root of the diffusion coefficient. Nevertheless, the present data do allow a comparison between two homologous series of probes of different polarity and our comblike polymer PMI-18 to be made. We will try to correlate in a semiquantitative way the apparent glass transition temperature for a given probe/PMI-18 system with the molecular characteristics of the probe in an effort to provide an insight into the influence of the free volume on the glass transition detection by IGC.

The free volume concept and Fujita equation have been used by Braun and Guillet[31] and have proved to be valuable empirical tools for the prediction of some characteristics of the retention diagrams as functions of operation conditions such as coating thickness, flow rate, polymer properties, etc. It is possible that a similar approach may well prove to be a reliable procedure to explain the dependence of our apparent glass transition temperatures on the size and polarity of the penetrating solute molecules.

Lower glass transition temperatures are associated with polymers having a large proportion of free volume in the rubbery state. According to the WLF theory[45] the free volume fraction $f_v(T)$ in a polymer at a temperature T above T_g can be conveniently expressed in the linear form

$$f_v(T) = f_v(T_g) + (\alpha_l - \alpha_g)(T - T_g) \qquad (16)$$

where $f_v(T_g)$ is the free volume fraction at the glass transition. It has the universal value of 0.025 for all polymers and $(\alpha_l - \alpha_g) = \Delta\alpha$ is the difference between the thermal expansion coefficients above and below T_g. This expression enables values of $f_v(T)$ to be calculated at any experimental temperature such as our apparent glass transition temperatures of Table III. The diffusion coefficient of a diffusate into a polymer matrix seems to depend on fractional volume and it can be given to a good approximation by Fujita's[46] equation in terms of our apparent glass transition temperatures through the free volume fraction by

$$D(T) = D_0 e^{-B/f_v(T)} \tag{17}$$

which relates the diffusion coefficient $D(T)$ to the fractional free volume $f_v(T)$. D_0 and B are two parameters depending on the polymer (D_0) and on the polymer and diffusate (B). They are assumed to be independent of temperature. D_0 may also denote the value of $D(T)$ at zero diffusate concentration. At higher concentration the diffusate makes a contribution to the free volume of the system and then eq 17 may no longer obtain.

The main problem of the diffusion in two-component systems is to estimate the mean diffusion coefficient $D(T)$—this coefficient in the Fujita equation is considered very often as a thermodynamic coefficient—of a given system from appropriate experimental data.

$D(T)$, though defined as a thermodynamic coefficient, may be considered as a mean diffusion coefficient and replaced by the mutual diffusion coefficient, $D(T) \simeq D^v$. The mutual diffusion coefficient D^v may be expressed[47,48] in terms of two intrinsic coefficients $\mathcal{D}_A$ and $\mathcal{D}_B$. When the partial volumes are constant they are related by the expression

$$D^v = V_A C_A(\mathcal{D}_B - \mathcal{D}_A) + \mathcal{D}_A \tag{18}$$

where C_A is the amount of component A contained in unit volume of the system and V_A is the constant volume of the unit amount of A used in the definition of the concentration. Usually, in solvent–polymer systems, $\mathcal{D}_B \ll \mathcal{D}_A$ and, therefore,

$$D^v = \mathcal{D}_A(1 - V_A C_A) = \mathcal{D}_A \phi_B \tag{19}$$

where ϕ_B is the mole fraction of the polymer and under our experimental conditions we can consider $\phi_B \simeq 1$, so in our case eq 19 takes the simple form of $D^v \simeq \mathcal{D}_A$, since the amount of probe within the polymer is almost zero. It is well-known that the IGC gives results with small concentrations of diffusates or rather lower volatility than is usual in sorption or permeation experiments.[49]

The intrinsic diffusion coefficient $\mathcal{D}_A$ can be related to the self-diffusion coefficient of component A, $\mathcal{D}^*_A$, by means of the following expressions:[47]

$$\mathcal{D}_A = \mathcal{D}^*_A C_A \frac{\delta\mu_A}{\delta C_A} = \frac{\mathcal{D}^*_A}{RT}\frac{\delta \ln a_A}{\delta \ln C_A} \tag{20}$$

where C_A, μ_A, and a_A denote the amount of component A contained in unit volume of the system, its chemical potential, and its thermodynamic activity, respectively. If we consider that the solution is ideal $\delta \ln a_A/\delta \ln C_A = 1$ and then

$$\mathcal{D}_A \simeq \mathcal{D}^*_A/RT \tag{21}$$

therefore all the above approximations lead to a series of relationships between different coefficients of diffusion, namely,

$$D(T) \simeq D^v \simeq \mathcal{D}_A \simeq \mathcal{D}^*_A/RT \tag{22}$$

from the first and last equalities we obtain $D(T) \simeq \mathcal{D}^*_A/RT$.

The self-diffusion coefficient $\mathcal{D}^*_A$ can be easily obtained by means of the following expression:[50]

$$\mathcal{D}^*_A = 1.20\frac{RT}{M}\frac{\Omega_V}{\Omega_D}\eta_A \tag{23}$$

where η_A is the viscosity in poise. The ratio Ω_V/Ω_D is a weak function of T^* ($T^* = kT/\epsilon$, and ϵ = potential energy parameter) and is approximately 1.1 at ordinary temperatures. Values for this ratio are tabulated for nonpolar as well as polar molecules. However, it is believed that the relation between $\mathcal{D}^*_A$ and η_A is almost independent of the choice of force law model and potential function (Lennard-Jones or Stockmayer).[50] M is the molecular weight and T the absolute temperature. In making a crude assumption, the viscosity η_A for a rigid noninteracting sphere model is

$$\eta_A = 26.69M^{1/2}T^{1/2}/\sigma^2 \tag{24}$$

where σ = hard-sphere diameter in angstroms. Values of σ for nonpolar molecules can be calculated from the relation of σ to critical constants through the equation

$$\sigma = (2.44 - \omega')(T_c/P_c)^{1/3} \tag{25}$$

where ω' is the acentric factor which is defined as[51]

$$\omega' = 0.006R + 0.02087R^2 - 0.00136R^3 \tag{26}$$

and R is the radius of gyration in angstroms. Values for R were taken from Reid, Prausnitz, and Sherwood.[50]

For polar molecules σ can be calculated by means of the potential function given by Stockmayer.[52] Brokaw[53] suggests that σ for polar molecules may be estimated as follows:

$$\delta = \frac{1.94 \times 10^3\ \mu_p^2}{V_b T_b} \tag{27}$$

$$\sigma = (1.585V_b/1 + 1.3\delta^2)^{1/3} \tag{28}$$

where σ is in angstroms, T_b the boiling point (K), μ_p the dipole moment (D), and V_b the liquid molal volume at the boiling point (cm^3/mol).

According to all the assumptions and simplifications we have made, the $D(T)$ coefficient can be finally expressed in terms of our apparent glass transition temperatures T_g's, the free volume of the polymer at this temperature $f_v(T)$, the molecular weight of the probe M, and the Lennard-Jones (n-alkanes) or Stockmayer (n-alkyl alcohols) potential parameter σ, for every series as

$$\ln D(T) = \ln (35.23 \times 10^{-6}\ T^{1/2}/M^{1/2}\sigma^2) = \ln D_0 - B/f_v(T) \tag{29}$$

So, if we plot $\ln D(T) = \ln (35.23 \times 10^{-6}\ T^{1/2}/M^{1/2}\sigma^2)$ versus $1/f_v(T)$ we will obtain a straight line of slope $-B$ and intercept $\ln D_0$ from which the coefficient at zero diffusate concentration D_0 may be obtained.

The $D(T)$ values from Table III are plotted in Figure 8, where two series of separate points have been calculated from the σ data by using eq 25 and 26 for n-alkanes and eq 27 and 28 for n-alkyl alcohols. Considering the assumptions and approximations and mainly the different sources used for the physicochemical constants of n-alkanes and n-alkyl alcohols, the agreement is quite good. The intercept and slope give values of 2.48×10^{-7} for D_0 and 5.66×10^{-2} for B. These two values compare well with the figures obtained for some other systems.[55,56] In view of the present results, the introduction of the free volume

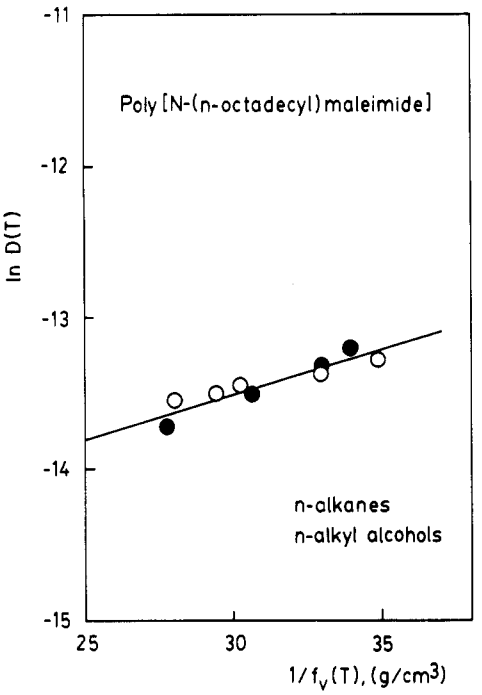

Figure 8. $\ln D(T) \simeq \ln (\mathcal{D}^*/RT)$ plotted against $1/f_v(T)$ for the diffusion of *n*-alkanes and *n*-alkyl alcohols in PMI-18. $D(T)$ in cm^2/s.

concept to explain the apparent glass transition temperture seems to be particularly successful in the description of the effects of chain length and polarity of probes and in their detection by IGC.

Concluding Remarks

The main conclusions derived from the present experimental data can be summarized as follows: (a) There is close agreement between heat of vaporization values for solutes *n*-alkanes and *n*-alkyl alcohols obtained by a GLC dynamic method (IGC) and those obtained from static vapor pressure/temperature data (Clausius–Clapeyron equation). (b) The thermodynamic information furnished by GLC on our comblike poly[*N*-(*n*-octadecyl)maleimide] (PMI-18) with two homologous series of nonpolar and polar solutes used as probes has been very useful to confirm the information on how the *n*-alkyl side chains of comblike polymers interact with *n*-alkyl chain derivatives. (c) The Fujita and Williams–Landel–Ferry equations are able to explain the order of magnitude of the differences found for the apparent glass transition temperature obtained from IGC using *n*-alkanes and *n*-alkyl alcohols as molecular probes.

Acknowledgment. We are grateful to the Consejo Superior de Investigaciones Cientificas and to the Curisión Asesora de Investigación Científica of the Ministerio de Universidades e Investigación for partial support of this research. We thank Prof. Dr. J. J. Freire, Department of Physical Chemistry, Universidad Courplutease of Madrid, for bringing ref 51 to our attention.

Registry No. PMI-18, 26714-93-2; nonane, 111-84-2; decane, 124-18-5; undecane, 1120-21-4; dodecane, 112-40-3; tridecane, 629-50-5; hexyl alcohol, 111-27-3; heptyl alcohol, 111-70-6; octyl alcohol, 111-87-5; decyl alcohol, 112-30-1.

References and Notes

(1) Lichtenthaler, R. N.; Liu, D. D.; Prausnitz, J. M. *Macromolecules* **1974**, *7*, 565.
(2) Lichtenthaler, R. N.; Prausnitz, J. M. In *Midland Macromolecular Monographs*; Solc, K., Ed.; Gordon and Breach: London, 1976; Vol. 2, p 67.
(3) Braun, J. M.; Guillet, J. E. *Macromolecules* **1975**, *8*, 557.
(4) Lichtenthaler, R. N.; Prausnitz, J. M.; Su, C. S.; Schreiber, H. P.; Patterson, D. *Macrmolecules* **1974**, *7*, 136.
(5) Card, T. W.; Al-Saigh, Z. Y.; Munk, P. *Macromolecules* **1985**, *18*, 1030.
(6) Braun, J.-M.; Guillet, J. E. *J. Polym. Sci., Polym. Chem. Ed.* **1975**, *13*, 1119.
(7) Braun, J.-M.; Guillet, J. E. *J. Polym. Sci., Polym. Chem. Ed.* **1976**, *14*, 1073.
(8) Schuster, R. H.; Gräter, H.; Cantow, H.-J. *Macromolecules* **1984**, *17*, 619.
(9) Al-Saigh, Z. Y.; Munk. P. *Macrmolecules* **1984**, *17*, 803.
(10) Gray, D. G.; Guillet, J. E. *J. Polym. Sci., Polym. Lett. Ed.* **1974**, *12*, 231.
(11) Barrales-Rienda, J. M.; Romero Galicia, C.; Horta, A. *Macromolecules* **1983**, *16*, 932.
(12) Barrales-Rienda, J. M.; Fernandez Martin, F.; Romero Galicia, C. *J. Macromol. Sci.—Phys.* **1984**, *B23*, 93.
(13) Ettre, L. S. *Open Tubular Columns in Gas Chromatography*; Plenum: New York, 1965.
(14) Mon, T. R. *Res. Develop.* **1971**, *22*, 14.
(15) Pella, E.; Nebuloni, M. *J. Thermal Anal.* **1971**, *3*, 229.
(16) Patterson, D.; Tewari, Y. B.; Schreiber, H. P.; Guillet, J. E. *Macromolecules* **1971**, *4*, 356.
(17) Littlewood, A. B.; Phillips, C. S. G.; Price, D. T. *J. Chem. Soc.* **1955**, 1480.
(18) Boublík, T.; Fried, V.; Hála, E. *The Vapour Pressures of Pure Substances. Selected Values of the Temperature Dependence of the Vapour Pressures of Some Pure Substances in the Normal and Low Pressure Region*; Elsevier: Amsterdam–New York, 1973.
(19) Orwoll, R. A.; Flory, P. J. *J. Am. Chem. Soc.* **1967**, *89*, 6814.
(20) Timmermans, J. *Physico-Chemical Constants of Pure Organic Compounds*; Elsevier: New York, 1950; Vol. 1; *Ibid.*, **1965**; Vol 2.
(21) Costello, J. M.; Bowden, S. T. *Recl. Trav. Chim. Pays-Bas* **1958**, *77*, 36.
(22) Selected Values of Properties of Chemical Compounds; Manufacturing Chemists Association Research Project; Texas A&M University, College Station, TX, 1966.
(23) McGlashan, M. L.; Potter, D. J. B. *Proc. R. Soc. London, Ser. B* **1962**, *267*, 478.
(24) Dreisbach, R. R. *Physical Properties of Chemical Compounds*; Advances in Chemistry; American Chemical Society: Washington, DC, 1959.
(25) Pitzer, K. S.; Curl, R. F. *J. Am. Chem. Soc.* **1957**, *79*, 2369.
(26) Barrales-Rienda, J. M.; González Ramos, J.; Sánchez Chaves, M. *Br. Polym. J.* **1977**, *9*, 6.
(27) Huggins, M. L. *J. Chem. Phys.* **1941**, *9*, 440.
(28) Flory, P. J. *J. Chem. Phys.* **1941**, *9*, 960.
(29) Barrales-Rienda, J. M.; Romero Galicia, C.; Freire, J. J.; Horta, A. *Macromolecules* **1983**, *16*, 1707.
(30) Braun, J.-M.; Guillet, J. E. *Macromolecules* **1975**, *8*, 882.
(31) Braun, J.-M.; Guillet, J. E. *Macromolecules* **1976**, *9*, 617.
(32) Braun, J.-M.; Guillet, J. E. *Macromolecules* **1976**, *9*, 340.
(33) Klein, J.; Waltnitzki, G. *Polym. Bull.* **1979**, *1*, 451.
(34) Ito, K.; Usami, N.; Yamashita, Y. *Macromolecules* **1980**, *13*, 216.
(35) Martin, R. L. *Anal. Chem.* **1961**, *33*, 347.
(36) Di Paola-Baranyi, G.; Guillet, J. E. *Macromolecules* **1978**, *11*, 228.
(37) Patterson, D.; Tewari, Y. B.; Schreiber, H. P. *J. Chem. Soc., Faraday Trans. 2* **1972**, *68*, 885.
(38) Couchon, M.; Phuong-Nguyen, H.; Delmas, G. *Can. J. Chem.* **1978**, *56*, 2472.
(39) Platé, N. A.; Shibaev, V. P. *J. Polym. Sci., Macromol. Rev.* **1974**, *8*, 117.
(40) Phuong-Nguyen, H.; Delmas, G. *Macromolecules* **1979**, *12*, 741.
(41) Flory, P. J. *Principles of Polymer Chemistry*; Cornell University Press: Ithaca, NY, 1953.
(42) Patterson, D. *Rubber Chem. Technol.* **1967**, *40*, 1.
(43) Guillet, J. E.; Galin, M. *J. Polym. Sci., Polym. Lett. Ed.* **1973**, *11*, 233.
(44) Belousov, V. G.; Kotsev, B. K.; Mikitayev, A. K. *Vysokomolekul. Soyed.* **1984**, *A26*, 1781; *Polym. Sci. USSR (Engl. Transl.)* **1984**, *26*, 1995.
(45) Williams, M. L.; Landel, R. F.; Ferry, J. D. *J. Am. Chem. Soc.* **1955**, *77*, 3701.
(46) Fujita, H.; Kishimoto, A.; Matsumoto, K. *Trans. Faraday Soc.* **1960**, *56*, 424.
(47) Crank, J.; Park, G. S. *Diffusion in Polymers*; Academic: New York, 1968.
(48) Crank, J. *The Mathematics of Diffusion*, 2nd ed.; Clarendon: Oxford, 1975.
(49) Gray, D. G.; Guillet, J. E. *Macromolecules* **1973**, *6*, 223.

(50) Reid, R. C.; Prausnitz, J. M.; Sherwood, T. K. *The Properties of Gases and Liquids*, 3rd ed.; McGraw-Hill: New York, 1976.
(51) Dymon, J. H.; Cholinski, J. A.; Szafranski, A.; Wyrzykowska-Stankiewicz, D. *Fluid Phase Equilib.* **1986**, *27*, 1.
(52) Stockmayer, W. H. *J. Chem. Phys.* **1941**, *9*, 398.
(53) Brokaw, R. S. *Ind. Eng. Chem. Process Des. Dev.* **1969**, *8*, 240.
(54) Mc Clellan, A. L. *Tables of Experimental Dipole Moments*; Rehera Enterprises: California, 1974; Vol. 2.
(55) Newns, A. C.; Park, G. S. *J. Polym. Sci., Polym. Symp.* **1969**, *22*, 927.
(56) Moisan, J. Y. In *Polymer Permeability*; Comyn, J., Ed.; Elsevier: London, 1986; pp 119-176.

Origins of Entanglement Effects in Rubber Elasticity†

Douglas Adolf

Sandia National Laboratories, Albuquerque, New Mexico 87185. *Received May 12, 1987*

ABSTRACT: The effects of entanglements on a network chain with fixed ends are modeled as hoops through which the chain must pass. This model differs from the tube models which allow no "chain leakage" from the tube and from the slip-link models which do not conserve monomer along the chain. The strain-dependent portion of the free energy as the chain ends are displaced is shown to arise from three factors: the entropy of the strained unentangled subchains spanning the hoops, the distortion of the hoops with strain, and the narrowing of the distribution of segments required to reach a hoop with increasing extension ratio. An analytical expression for the free energy of the chain can be derived that takes the $M - 1$ hoops per chain to be of infinitesimal diameter thereby neglecting this second factor. The resulting free energy for a network of these chains is of the form

$$A = (\xi/2)[M\sum_1^3 \lambda_i^2 + (M-1)\ln \sum_1^3 \lambda_i^2]$$

where ξ is the cycle rank of the network and λ_i is the extension ratio along the ith axis.

The early theories of rubber elasticity due to Flory[1] and James and Guth[2] allowed network chains to pass through each other freely and gave expressions for the force in response to a uniaxial deformation of the form

$$f \sim (\lambda - 1/\lambda_2) \quad (1)$$

where λ is the extension ratio. However, it is well-known[3] that the reduced force

$$[f^*] = f/(\lambda - 1/\lambda^2) \quad (2)$$

is not independent of the uniaxial extension ratio. Recent molecular theories have attributed this effect to the conservation of network topology via entanglements but have modeled the entanglements in several different ways. The constrained junction theories of Floy and Erman[4,5] and Ronca and Allegra[6] assume that the major effect of entanglements is to modify the strain dependence of the network junction fluctuations. The tube models of Gaylord[7] and Marrucci[8] assume that the network chains are confined to virtual tubes by the entanglements. Finally, the theories of Edwards and co-workers[9,10] model the entanglements by slip-links that preserve network topology. In the present model, entanglements acting on a single polymer chain are envisioned simply as hoops through which the chain must pass. This view is not as restrictive as confining the chain to a tube and, as shown later, differs from the slip-link model in that it does not consider subchains connecting sliplinks to be individual entities each with a prescribed length distribution.

Theory

A simple version of this model is shown in Figure 1 where the chain endpoints are located at (0,0,0) and (0,0,z) and the $M - 1$ hoops are equally spaced squares perpendicular to and centered about the z axis. The partition function for the chain can be expressed as

$$Q = \int_0^N dn_1 \int_{-\infty}^{\infty} dx_1 \int_{-\infty}^{\infty} dy_1 \, F(x_1)F(y_1)G(x_1-x_0,y_1-y_0,H,n_1) \int_0^{N-n_1} dn_2 \int_{-\infty}^{\infty} dx_2 \int_{-\infty}^{\infty} dy_2 \, F(x_2)F(y_2)G(x_2-x_1,y_2-y_1,H,n_2) \ldots \quad (3)$$

where $G(x,y,H,n)$ is the probability that a subchain connecting two entanglements (hoops) and starting at the origin will end at (x,y,H) in n segments. The partition function is an M-fold convolution in the chain-length variable which results from the fact that each of the subchains requires n_i segments to reach the next hoop and $\sum_1^M n_i$ must equal N, the total number of segments of length l on the chain. If the chain statistics are assumed to be Gaussian, then G is given by

$$G = (3/2\pi n l^2)^{3/2} \exp[-3(x^2 + y^2 + H^2)/2nl^2] \quad (4)$$

$F(x)$ defines the size of the hoop along the x axis and may be, for example, a repulsive hard core or a harmonic potential. For the case of a hard core potential, $F(x) = 1$ for $-a \le x \le a$ and 0 elsewhere for a square hoop of width $2a$.

Mathematically, the simplest function for $F(x)$ is the Dirac δ function, $\delta(x)$, for which the hoop diameter vanishes. Using this, the spatial integrations are easily evaluated and the partition function can be evaluated by Laplace transformation of the convolution in N and subsequent inversion. The resulting expression for the partition function is in this case

$$Q = \frac{K(M,l,N)}{H^{M-1}} \exp(-3M^2H^2/2Nl^2) \quad (5)$$

where K is a function independent of the extension ratio. If we make the assumption that the position of an entanglement (hoop) deforms affinely when the chain end is moved from z to λz, then $H = \lambda H_0$. Using the formula f

†This work performed at Sandia National Laboratories supported by the U. S. Department of Energy under Contract DE-AC04-76DP00789.

0024-9297/88/2221-0228$01.50/0